Journal Pre-proofs

A PTFE helical capillary microreactor for the high throughput synthesis of monodisperse silica particles

Hui Yang, Eser Metin Akinoglu, Lijing Guo, Mingliang Jin, Guofu Zhou, Michael Giersig, Lingling Shui, Paul Mulvaney

Please cite this article as: H. Yang, E. Metin Akinoglu, L. Guo, M. Jin, G. Zhou, M. Giersig, L. Shui, P. Mulvaney, A PTFE helical capillary microreactor for the high throughput synthesis of monodisperse silica particles, *Chemical Engineering Journal* (2020), doi: https://doi.org/10.1016/j.cej.2020.126063

This is a PDF file of an article that has undergone enhancements after acceptance, such as the addition of a cover page and metadata, and formatting for readability, but it is not yet the definitive version of record. This version will undergo additional copyediting, typesetting and review before it is published in its final form, but we are providing this version to give early visibility of the article. Please note that, during the production process, errors may be discovered which could affect the content, and all legal disclaimers that apply to the journal pertain.

A PTFE helical capillary microreactor for the high throughput synthesis of monodisperse silica particles

Hui Yang[1,2], Eser Metin Akinoglu[3,1,*], Lijing Guo[1], Mingliang Jin[1], Guofu Zhou[1,2], Michael Giersig[1,4], Lingling Shui[1,5], Paul Mulvaney[3,1]

[1] *International Academy of Optoelectronics at Zhaoqing, South China Normal University, Zhaoqing, 526238 Guangdong, P. R. China*

[2] *Guangdong Provincial Key Laboratory of Optical Information Materials and Technology & Institute of Electronic Paper Displays, South China Academy of Advanced Optoelectronics, South China Normal University, Guangzhou 510006, P.R. China*

[3] *ARC Centre of Excellence in Exciton Science, School of Chemistry, University of Melbourne, Parkville, VIC, 3010, Australia*

[4] *Institute of Fundamental Technological Research, Polish Academy of Sciences, 02-106 Warsaw, Poland*

[5] *School of Information and Optoelectronic Science and Engineering, South China Normal University, Guangzhou, 510006 Guangdong, P. R. China*

Abstract

We propose a simple and inexpensive SiO_2 submicron particle synthesis method based on a PTFE helical capillary microreactor. The device is based on Dean flow mediated, ultrafast mixing of two liquid phases in a microfluidic spiral pipe. Excellent control of particle size between 100 nm and 600 nm and narrow polydispersity can be achieved by controlling the device and process parameters. Numerical simulations are performed to determine the optimal device dimensions. In the mother liquor the silica particles exhibit zeta potentials < -60mV, rendering them very stable even at high particle volume fractions. The current device typically produces around 0.234 g/h of the silica particles.

Keywords: SiO_2 particle synthesis, continuous flow synthesis, helical capillary microreactor

1. Introduction

Since Stöber first reported on the synthesis of solid silica micro-/nanoparticles by means of hydrolysis of alkyl silicates and subsequent condensation of silanols and silicic acid in alcoholic solution in 1968, there has been enormous interest in the synthesis of silica based nanomaterials.[1] Both solid and porous silica materials have been reported and their good biocompatibility, high thermal and mechanical stability and ease of surface functionalization have all been exploited in many applications.[2] Traditionally, such silica particles have been synthesized in a batch-wise manner to obtain large quantities. Micro-structured chemical reactors provide a useful alternative to batch reactors because they offer better control over the reaction rate.[3] Here we use a helical tubular microreactor for the high throughput synthesis of monodisperse submicron silica particles. We exploit Dean's flow to achieve both high throughput and sorting efficiency.[4,5] Under Dean's flow [6] the magnitude of the main stream velocity in a curved channel at the outer (larger radius) side of the channel is larger than that at the inner wall.[5] The difference in the speed of the fluids along the opposing channel walls is accompanied by a pressure gradient in the radial direction, which results in a secondary flow driving the fluid from the inner wall to the outer wall of the channel and this, in turn, leads to travelling vortices.[7] This effect can be utilized to achieve ultrafast mixing of two adjacent liquid phases in a single spiral microchannel.

In general, there are two types of spiral microchannel reactors, using either planar or helical geometry. Planar spiral microreactors are typically fabricated using lithographic methods and these reactors have indeed been used for the synthesis of silica particles in the past. For example, Yuan Nie et al. demonstrated a lithographically fabricated microfluidic spiral channel device for the synthesis of submicron, hollow, silica spheres.[8] This geometry has also been used for solid-forming reactions,[9,10] ultra-fast blood plasma separation,[11] and manipulation

of biological particles.[12,13] Though elegant, such devices require an extensive sequence of fabrication steps and necessitate photolithography for assembly.[14] In particular, the bonding of multiple device layers requires tedious micro-scale alignment and surface treatments, which all render commercialization difficult and expensive. Furthermore, these devices are usually based on polydimethylsiloxane (PDMS) and glass-based chips, which have intrinsically poor heat conductivity making uniform heating within the device difficult. Also, the small chip sizes amenable to photolithography make it difficult to achieve sufficiently large residence times. Hence, the complexity of the devices and the associated fabrication constraints limit its applicability severely. On the other hand, helical tubular microreactors offer improved heat and mass transport as well as enhanced mixing compared to planar spiral microreactors.[15] Mixing takes place along the length of the microreactor in planar micro-structured reactors, whereas the mixing occurs along the length of the microreactor as well as in the radial direction in the helical capillary micro-reactor.[16,17] The efficiency of helical tubular microchannel reactors has been validated using the synthesis of Ag nanoparticles (NPs),[18] peracetic acid,[19] and peroxypropionic acid.[20]

Here, we propose to use this facile and inexpensive method to produce uniform SiO_2 particles with controlled sizes between 100 nm and 600 nm diameter and yields up to 0.234 g/h of solid product. We achieve this with a lithography-free, microfluidic device based on a polytetrafluoroethylene (PTFE) spiral microchannel. In this device, two fluid phases undergo ultrafast mixing due to Dean flow effects. The two adjacent fluid phases consist of the silica precursor, TEOS, in a non-aqueous solvent and $NH_3 \cdot H_2O$ as the catalyst in the aqueous phase. Hydrolysis of TEOS and its continuous condensation during the mixing of the two reactant flows leads to the build-up of nanoparticles in the spiral microchannel.[21] Numerical analysis is used to optimize the device dimensions in order to obtain complete mixing in less than 1.4 s.
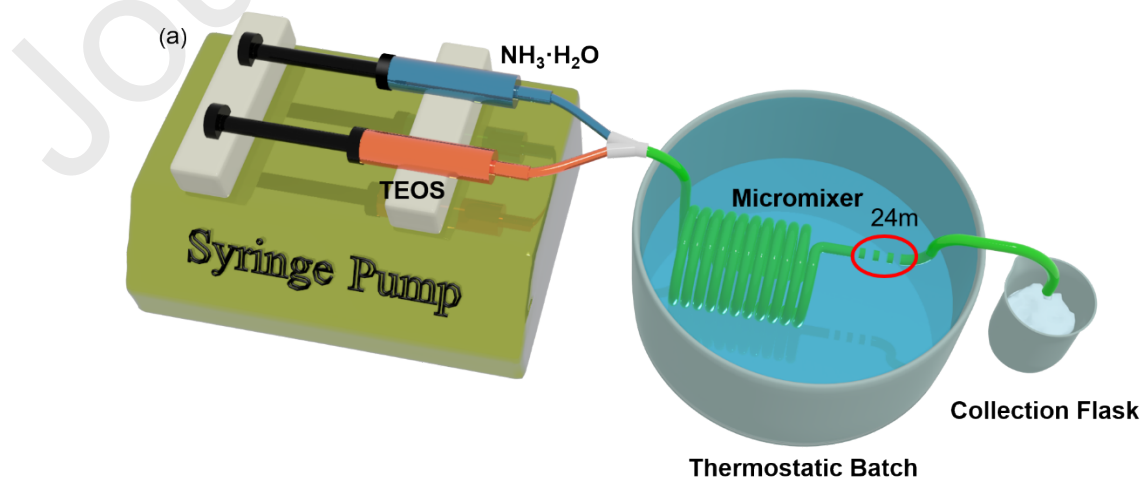
2. Experimental Section

2.1 Materials

Tetraethyl orthosilicate (TEOS), ammonium hydroxide solution (28%) and dry ethanol were purchased from Aladdin, Shanghai, China. 18 MΩ ultrapure Milli-Q water was used for all experiments. All chemicals were used as received without any further purification.

2.2 Fabrication of microfluidic devices

The micromixer consists of a 0.5 m long polytetrafluoroethylene (PTFE) tube with an inner diameter of 0.8 mm and an outer diameter of 1.6 mm, which is wrapped around a glass rod with 6 mm diameter. At the entrance, a Y-shaped mixer connects the PTFE tube to two silicone hoses with matching inner diameters, which are the injection points for liquid from separately controlled syringe pumps. For this synthesis a well-defined constant temperature and sufficient residence time is required to ensure good SiO_2 particle growth. We achieve this by placing this microchannel reactor into a heat bath and use a PTFE tube extension of 24 m to ensure sufficiently long residence times (30 min.) for particle growth. Control over the process is maintained with the syringe pumps, by manipulating the flow rates of the two liquid phases that are being injected.
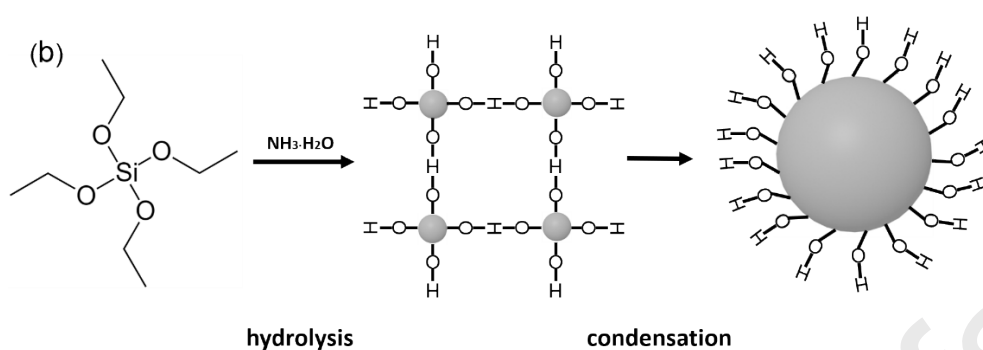
Figure1 : (a) Experimental set-up of the microfluidic mixer for (b) the continuous synthesis of SiO$_2$ particles.

2.3 SiO$_2$ particle synthesis and characterization

TEOS hydrolyzes in ethanol in the presence of aqueous ammonia as a catalyst, which results in the formation of silanols. These silanols condense with either TEOS or other silanols. Continued hydrolysis of the ethoxy groups and subsequent condensation results in crosslinking, forming silica oligomers and eventually small particles.[22] Whether the silica surface undergoes adsorption or surface modification by a silane coupling agent depends upon the chemistry of the hydroxyl groups on its surface.[23] The surface is usually assumed to comprise silanol groups S—OH and siloxane groups (Si-O-Si). The silanol groups render the silica hydrophilic and these moieties can also act as centres for further electrostatic and chemical interaction. However, siloxane groups are chemically more inert and render the surface hydrophobic; the adsorption capacity of the particles also becomes weaker, thus stopping the growth of the silica particles.[24] A solution of 10 mL ammonia water in 20 mL pure ethanol was prepared. TEOS in pure ethanol was prepared by pipetting 2 mL TEOS into 32 mL pure ethanol. The two reactant solutions were then ultrasonically treated for 10 min and introduced into the syringes before entering the microfluidic spiral at a speed of 400 µL/min, if not otherwise specified. The micromixer was placed into a thermostatted solvent bath at an arbitrary but constant temperature. The exiting, mixed solution was kept flowing in the extended PTFE tube to prolong the residence time and

enable SiO_2 particle growth. Finally, the NPs were isolated from the solution by centrifugation for 5 min at 5600 g and redispersed in purified water several times to remove excess ammonia and then dried in a vacuum desiccator for 24 h. However, the silica particles are also stable without purification and can be stored as synthesized. A ZEISS Sigma 500 scanning electron microscope (SEM) was used to determine the particle uniformity and size, for which at least 300 particles were measured. A Brookhaven NanoBrook Omni instrument was used to obtain the zeta potential of the particles at pH = 6.8. For this the electrophoretic mobility μ_{ep} of the suspension was measured and converted to zeta potential ζ via the relation $\mu_{ep} = \varepsilon_r \, \varepsilon_0 \, \zeta / \, \eta$, where ε_r is the relative permittivity, ε_0 is the vacuum permittivity and η is viscosity of the liquid. Because of the low dielectric constant of the solvent and low electrolyte concentration, the Hückel approximation was used. The product yield was calculated by weighing the dried particle suspension that was synthesized over a fixed time of 20 min.

2.4 Simulations of the microfluidic device
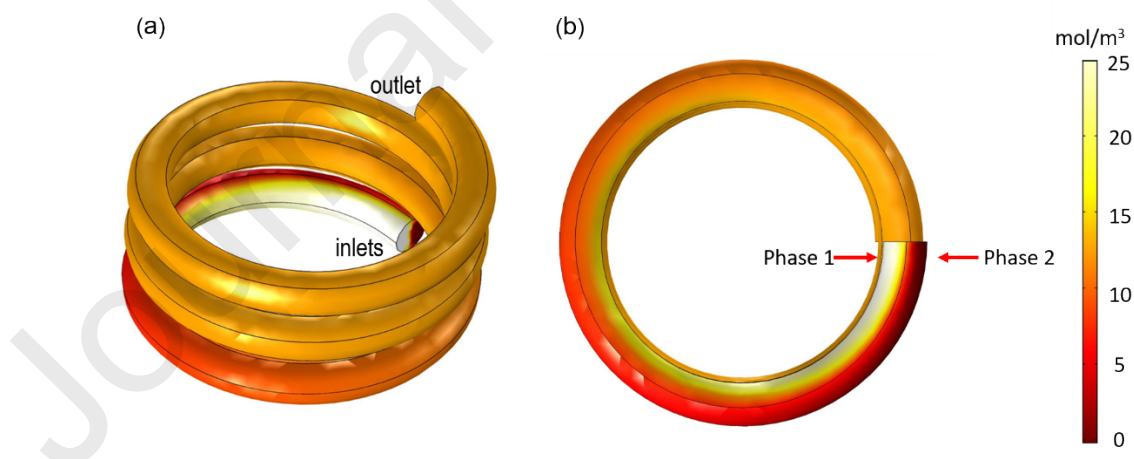
Figure 2. Simulation of the spiral microreactor. (a) A side perspective showing the microreactor with inlets and outlets. (b) a top view along the spiral axis to illustrate the two distinct phases that are introduced into the inlet. The concentration gradient represented by the colour gradient from white to red is shown in the colour bar. As the two phases move along the spiral, fast mixing occurs and the two phases merge into a single phase after one run. Here $d_p =$ is 0.8 mm, d_R = 6 mm, and the total flow rate is 400 μL/min.

Micromixing in the microfluid spiral was simulated with the COMSOL 5.3a Fluid Flow module in a 3D geometry. The model uses the Laminar Flow module and the Transport of Diluted Species module. The physics is governed by the Navier-Stokes equations with *no slip* boundary conditions and the gravity force was neglected. Fully developed laminar flow is assumed at the inlet and a pressure of zero is set at the outlet. The boundary condition of the two phases at the inlet is defined by a step function where the pipe is divided in the middle to a phase with initial concentration c_0 and another phase with an initial concentration of 0. Mixing was evaluated from the concentration profiles from cross-sectional slices of the spiral. Because the silica formation process takes as long as 30 min, while the residence time inside the spiral channel is less than 40 s, the silica particle growth occurs mostly after passing through the micromixer. Hence a constant density and velocity is assumed particle generation inside the spirals is not considered. The fluids were simulated as pure water and water with some dissolved species of diffusion coefficient D = 4.5 x 10^{-9} m^2/s and the dynamic viscosity of water was assumed to be ρ = 0.001 Pa·s. This is shown in Figure 2a as two distinct colours, i.e. white and dark red. A top view of the computational cell is shown in Figure 2b. Their flow rates were set at 400 μL/min. As the fluids travel along the channel, mixing occurs as shown in Figure 2. This occurs because Dean instabilities are generated, which result in a pressure and velocity gradient imbalance and this results in vortices, defined by the Dean number (*De*):

$$De = Re\sqrt{\frac{D_h}{2R}} = 3.85 \quad Re = \frac{\rho v D_h}{\mu} = 10.54$$

Here, ρ is the density of H$_2$O at 20 °C (998 kg/m^3), D_h is the hydraulic diameter of the pipe (0.8x10-3 m), v is the mean velocity of the object relative to the fluid (m/s) given by v = (flow rate)/(cross section area) = 0.0132 m/s, μ is the viscosity of H$_2$O (1x10-3 Pa·s), *R* is the flow path radius of the curvature (3 x10^{-3} m) and *Re* is Reynolds number[25].

3 Results

3.1 Simulation of device dimensions

Computational analysis is used to determine how many turns in the helical capillary micromixer are required for complete mixing of the two liquid phases. In the laminar flow region, a parabolic velocity pattern within a capillary microreactor can be obtained through introduction of curved channels. This can be achieved by wrapping a flexible straight capillary around a cylindrical rod-shaped core. The perturbations induced by the centrifugal forces act perpendicularly to the fluid flow direction inside the spirals. Consequently, a secondary flow pattern is induced in the circular cross section of the capillary micro-reactor, which promotes mixing. The mixing efficiency can be studied by determining at which point complete mixing is achieved along the helical microchannel. Our model employed a flow rate of 400 μL/min and constant rod diameter d_R =

0.6 cm, around which a helical microchannel with variable channel diameter d_P was wound. We varied d_P from 0.5 mm to 2 mm and found that a monotonous and roughly linear increase in the number of spiral turns was required to achieve complete mixing. This is expected because, for a constant flow rate, the diameter of the channel is inversely proportional to the flow velocity inside the channel. The effect of d_R, which determines the curvature of the channel is shown in Figure 3b. A constant flow rate of 400 μL/min and constant d_p = 0.8 mm were used and the channel diameter d_R was varied from 0.4 cm to 10 cm. Two distinct plateau regimes are observed and, in both of these regimes, the distance at which complete mixing was achieved remained roughly constant, i.e. for d_R = 0.4 cm to 1 cm a length of 1.96 cm was required and for d_R = 2 cm to 10 cm a length of 5.04 cm was required. This means that varying d_R from 4 mm to 10 mm did not affect the mixing.
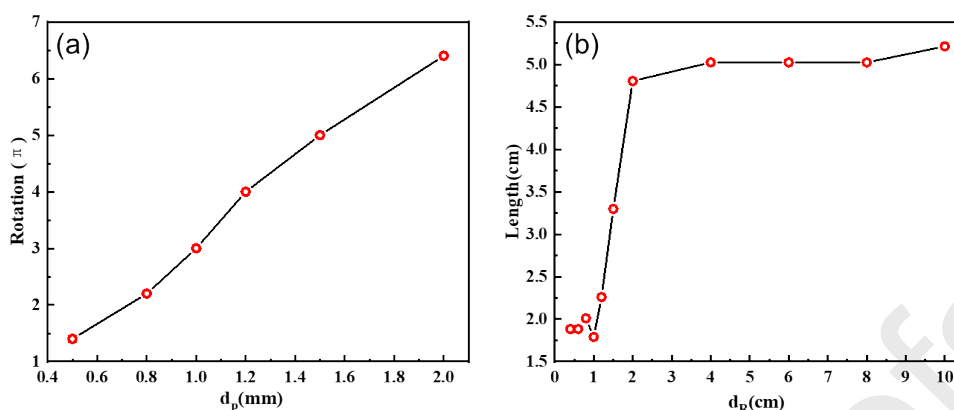
Figure 3. Point of complete mixing of two phases in a spiral microreactor. a) the number of turns required for complete mixing as a function of d_P for a fixed value of d_R = 0.6 cm. b) the mixer length required for complete mixing as a function of d_R for d_P = 0.8 mm. The flow rate of the two reactant phases in the pipe is 400 µL/min. The diffusion coefficient is D = 4.5 x 10^{-9} m/s, while the dynamic viscosity is that of water: ρ = 0.001 Pa·s.

For the experimental realization d_R = 0.6 cm and d_P = 0.8 mm were chosen, which should enable complete mixing after 1.43 s at an injection flow rate 400µL/min combined within the micromixer respectively. We have compared the silica particle synthesis for a device with these dimensions to that of the equivalent without a spiral geometry shown in Figure S1. Clearly, the micromixer produces a much more homogeneous size distribution, which we attribute to the ultra-fast mixing of the precursor phases.

3.2 c_{TEOS} dependence on SiO$_2$ particle growth

The effect of the TEOS concentration on the SiO$_2$ NP synthesis was studied by varying c_{TEOS} in the ethanol phase, while keeping all other parameters constant at c_{NH3} = 8.7mol/L, T = 40 °C, and the flow rate at 400 µL/min. SEM analysis (Figure 4a-d) reveals that the silica NP size dispersity is not affected but the silica NPs increase approximately linearly in mean diameter with increasing c_{TEOS} and this can be controlled, allowing the NP diameter to be tuned from 150 nm

to 500 nm (Figure 4e). Histograms showing the size distribution of these synthesized particles

are shown in Figure S2. Zeta–potential measurements yield ζ ~ -60 mV (Figure 4e).
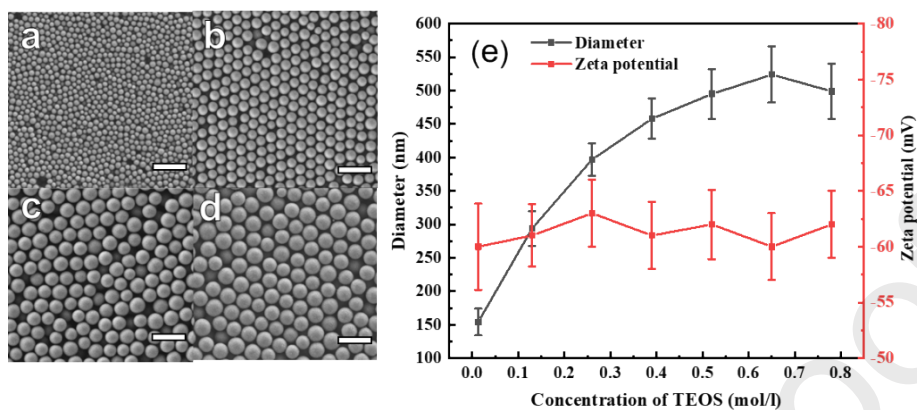
Figure 4. The dependence of SiO_2 particle growth on the concentration of TEOS in the ethanol phase. SEM images of SiO_2 particles with (a) 0.013 mol/L, (b)0.13 mol/L, (c) 0.26 mol/L, (d) 0.39 mol/L, (e) 0.52 mol/L, (f) 0.65 mol/L and (g) 0.78 mol/L TEOS concentration. The scalebar is 1 μm. The diameters and zeta potentials of the particles are shown in (e), where the first data point corresponds to a) and the last to d).

### 3.3 c_{NH3} dependence on SiO_2 particle growth

The effect of the ammonia concentration on the SiO_2 NP synthesis was studied by varying c_{NH3}

in the water phase. All other parameters were kept constant at c_{TEOS} = 0.26 mol/L, T = 40 °C,

and the flow rate at 400 µL/min. From the SEM analysis shown in Figure 5a-d it is evident that

the silica NP size is dramatically affected by c_{NH3}, ranging from 200 nm to 500 nm diameter

(Figure 5e). The growth is not linear but peaks at c_{NH3} = 13.05 mol/L followed by a decrease in

NP size for higher c_{NH3}. Simultaneously, the size homogeneity is lost and polydispersity

increases. Histograms showing the size dependence are presented in Figure S3. ζ-potential

analysis shows ζ < -60 mV in all cases, which ensures good colloidal stability of the synthesized

SiO_2 NPs.
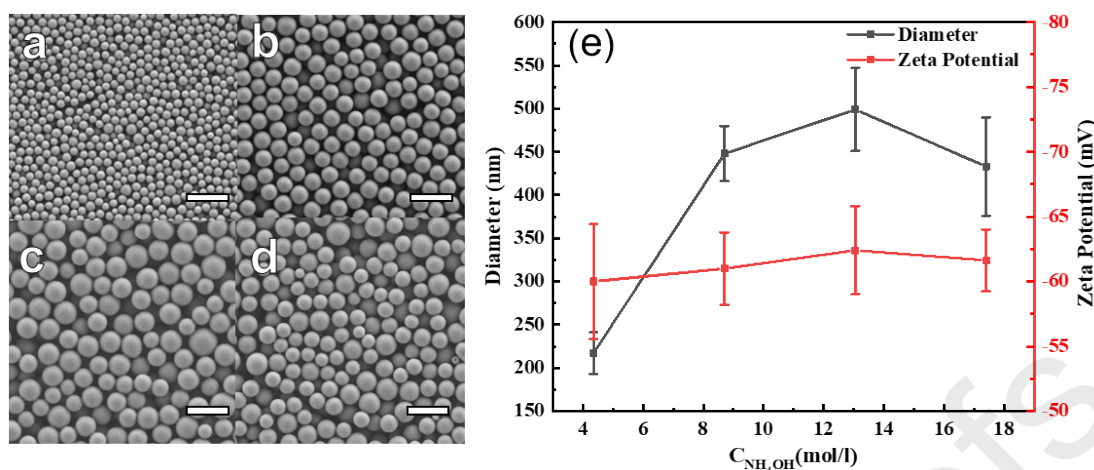
Figure 5. The dependence of SiO$_2$ particle growth on the concentration of NH$_3$·H$_2$O. SEM images of SiO$_2$ particles with (a) 4.35 mol/L, (b) 8.7 mol/L, (c) 13.05 mol/L, and (d) 17.4 mol/L NH$_3$·H$_2$O concentration. The scale is 1 μm. The diameters and zeta potentials of the particles are shown in (e).

### 3.4 Phase flow rate dependence on SiO$_2$ particle growth

The effect of the insertion flow rate on the silica NP synthesis was studied for flow rates ranging from 200 µL/min to 500 µL/min and SEM images of the resulting NPs are shown in Figure 6a-d. All other parameters were kept constant at c_{TEOS} = 0.26 mol/L, c_{NH3} = 8.7 mol/L, and T = 40 °C. The diameters of the silica NPs are found to differ in size between 390 nm and 480 nm with lower polydispersity for larger flow rates. The narrowest size distribution was found for a flow rate of 400 µL/min. Histograms showing the size dependence are presented in Figure S4. Again, we observed that the zeta potential ζ < -60 mV in all cases as shown in Figure 6e and was largely unaffected by the phase flow rates.
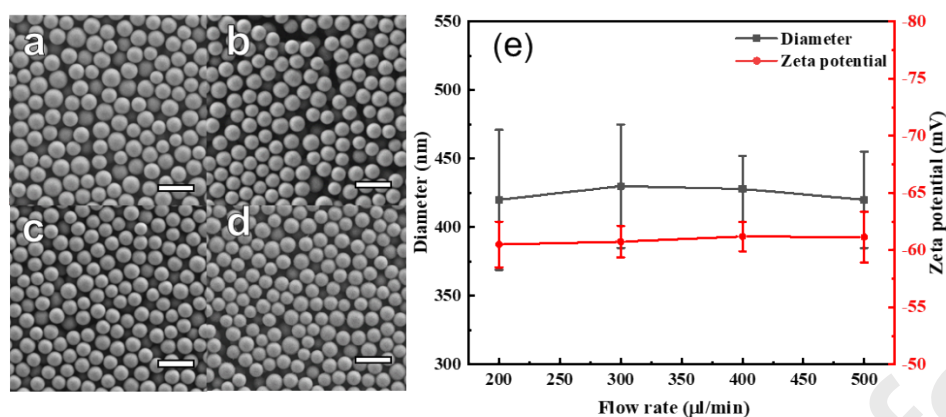
Figure 6. The dependence of SiO$_2$ particle size on the phase flow rates. (a) 200 μL/min; (b) 300 μL/min; (c) 400 μL/min; (d) 500 μL/min; The scalebar is 1μm.

3.5 Temperature dependence of the SiO$_2$ particle size

The reaction temperature is an important parameter and its effect on the silica NP synthesis was studied over the range from 30 °C to 60 °C. The phase flow rates were kept constant at 400 μL/min, while c_{TEOS} = 0.26 mol/L and c_{NH3} = 8.7 mol/L. The SEM images of the NPs synthesized under these conditions are shown in Figure 7a-d. We observed an approximately linear decrease in SiO$_2$ NP size with increasing temperature. At the same time, the size dispersity of the particles was reduced for higher T. Histograms showing the size dependence are presented in Figure S5.
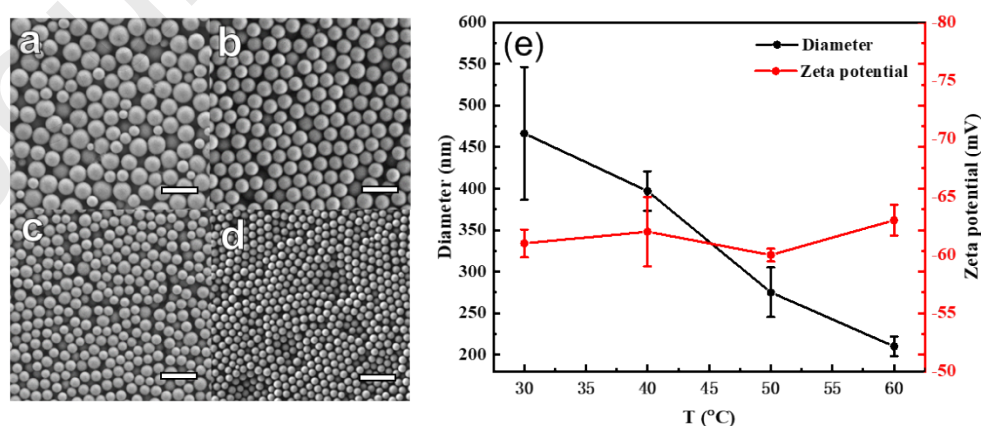
Figure 7. The dependence of SiO$_2$ particle size on the reactor temperature. SEM images of SiO$_2$ NPs

synthesized at (a) 30 °C, (b) 40 °C, (c) 50 °C, and (d) 60 °C. The scale bar is 1 μm. (e) The particle diameter and the zeta potential vs. reactor temperature with constant c_{TEOS} = 0.26 mol/L, c_{NH3} = 8.7 mol/L, and 400 μL/min phase flow rates.

3.6 Product yield

The solid product yield of the device was measured for a process using c_{TEOS} = 0.26 mol/L, c_{NH3} = 8.7 mol/L, T = 40 °C, a flow rate of 400 μL/min and a time of 20 min. For this the SiO$_2$ were dried and the yield was quantified in three separate measurements yielding a mean rate of production of silica of 0.23 ± 0.02 g/h.

4. Discussion

From the simulations we obtained information on the optimum micromixer dimensions. Because the Dean effect has a close relationship to both the pipe and rod radii, these parameters affect the mixing of the phases significantly.[26] The radius of the pipe affects the travel distance within the spiral linearly; in other words, the thinner the pipe, the higher the velocity, such that complete mixing is achieved more rapidly.[27,28] However, because a long residence time is required for complete reaction, higher velocities necessitate the use of longer pipes,[21] i.e. a 0.5 mm diameter pipe would require a total length of 64 m to obtain a residence time of 30 min at a flow rate of 400 μL/min to ensure full SiO$_2$ NP growth. Therefore, a diameter of 0.8 mm is more practical because it shortens the total required pipe length to 24 m. Conversely, for larger d_p = 1 mm, the velocity will decrease from 0.034 m/s at d_p = 0.5 mm to 0.0084 m/s which favours adhesion of particles to the side walls as well as particle agglomeration, and this will eventually lead to complete clogging of the channel. A change in the rod diameter d_R from 0.4 cm to 10 cm (at constant d_P = 0.8 mm) leads to two distinct plateau regimes during reaction, and within both of these regimes the reactor length required for complete mixing is roughly constant, i.e. for d_R

= 0.4 cm to 1 cm a length of 1.96 cm is required and for d_R = 2 cm to 10 cm a length of 5.04 cm is required. To achieve ultrafast mixing completely in short times, the parameters d_R = 0.6 cm and d_P = 0.8 mm were used throughout this study.[29] The final particle size depends on the rate of two processes, i.e the hydrolysis of TEOS which controls the initial nucleation of silica nuclei and the condensation of silanol groups, which enables the particles to grow.[1] The SiO_2 NP size depends linearly on the TEOS concentration (Figure 4), implying that condensation is more facile than nucleation. By tuning $c_{TEOS,}$ the size of the SiO_2 NPs can be controlled over the range from 100 nm to 600 nm. The ammonia concentration also affects the formation of SiO_2 NPs.[30] An increase in c_{NH3} increases the rate of hydrolysis process and the size of SiO_2 NPs also increases (Figure 5). Because the ammonia is introduced into the ethanol phase as an ammonium hydroxide solution, it also includes water.[31] An increase in the water volume initially increases the size of the SiO_2 NPs.[32] However, after a peak in particle size, the size decreases with further increases in the water volume.[33] A further decrease of the ammonia concentration could reduce polydispersity, but because of the implied slower reaction the particle growth cannot be concluded within the 30 min residence time in the device. For larger ammonia concentrations the reaction is very fast which results in clogging of the channel. Different flow rates, varying from 200-500 μL/min, had no significant effect on the size of the particles (Figure 6). This is readily

understood because under the conditions employed here, particle growth is governed by diffusion, and hydrodynamic effects can be neglected.[34] Larger flow rates increase the flow speed and required longer pipe length, which then become less practical. Smaller flow rates result in the aggregation of particles within the pipe leading to clogging. The most uniform particles were obtained at a flow rate of 400 μL/min. SiO_2 NP growth was also affected by the temperature, with an increase in T resulting in a decrease in the NP size (Figure 7). This is expected because a higher nucleation rate is known to lead to smaller mean particle sizes and also narrower size distributions.[35,36] It is important to consider that the reaction is performed

in ethanol with a boiling point of 78 °C so that an increase in temperature beyond 60°C is not feasible. On the other hand, temperatures below 30 °C are not feasible because the uniformity of the particles already decreases significantly at 30 °C. Overall, all the final silica particles consistently exhibit large negative zeta potentials, which explains the strong colloid stability. The above trends demonstrate that submicron silica particles can be produced in a spiral microreactor using the well-defined hydrodynamic conditions that prevail during Dean flow. Variation in reactor design allows submicron particles of different sizes to be produced with great uniformity (Figure S6). While protocols for uniform silica are well known, this work shows how chemical synthesis can be switched from batch-wise to continuous flow, while still allowing good control of particle size. In future work we will show that this simple system can be extended to allow doped silica particles to be created. The doping with fluorophores, magnetic dopants and general chromophores will be presented. The reactor design here lends itself for the fabrication of more complex morphologies and nanostructured colloids.

5. Conclusion

In conclusion, a new PTFE based helical capillary microreactor has been developed and optimized for submicron SiO2 particle synthesis. Dean flow effects in the curved channel enable ultrafast mixing of two phases, which we have exploited to synthesize SiO_2 particles based on the Stöber method. We have investigated the effect of different device geometries and process parameters on the SiO_2 NP synthesis and optimized the reaction conditions for preparation of uniform silica colloids. The TEOS concentration and reaction temperature are found to influence the particle size dramatically. Due to the simplicity of the device assembly and its high mixing efficiency, high product yields at remarkably low cost can be achieved. This micromixer could be used as a microfluidic platform for the synthesis of a range of uniform and nanostructure or doped particles.

Competing Interests

Acknowledgements

References

[1]   W. Stöber, A. Fink, E. Bohn, Controlled Growth of Monodisperse Silica Spheres in the Micron Size Range, J. Colloid Interface Sci. 26 (1968) 62–69.

[2]   N. Hao, Y. Nie, Z. Xu, A.B. Closson, T. Usherwood, J.X.J. Zhang, Microfluidic continuous flow synthesis of functional hollow spherical silica with hierarchical sponge-like large porous shell, Chem. Eng. J. 366 (2019) 433–438.

[3]   J.B. Wacker, I. Lignos, V.K. Parashar, M.A.M. Gijs, Controlled synthesis of fluorescent silica nanoparticles inside microfluidic droplets, Lab Chip. 12 (2012) 3111–3116.

[4]   A.A.S. Bhagat, H.W. Hou, L.D. Li, C.T. Lim, J. Han, Dean flow fractionation (DFF) isolation of circulating tumor cells (CTCs) from blood, 15th Int. Conf. Miniaturized Syst. Chem. Life Sci. 1 (2011) 524–526.

[5]   N. Nivedita, P. Ligrani, I. Papautsky, Dean Flow Dynamics in Low-Aspect Ratio Spiral

Microchannels, Sci. Rep. 7 (2017) 1–10.

[6]   W.R.Dean M.A, The stream-line motion of fluid in a curved pipe, London, Edinburgh, Dublin Philos. Mag. J. Sci. 5 (1928) 673–695.

[7]   M. Rafeie, M. Welleweerd, A. Hassanzadeh-Barforoushi, M. Asadnia, W. Olthuis, M.E. Warkiani, An easily fabricated three-dimensional threaded lemniscate-shaped micromixer for a wide range of flow rates, Biomicrofluidics. 11 (2017) 1–15.

[8]   Y. Nie, N. Hao, J.X.J. Zhang, Ultrafast Synthesis of Multifunctional Submicrometer Hollow Silica Spheres in Microfluidic Spiral Channels, Sci. Rep. 7 (2017) 1–9.

[9]   S. Kuhn, T. Noël, L. Gu, P.L. Heider, K.F. Jensen, A Teflon microreactor with integrated piezoelectric actuator to handle solid forming reactions, Lab Chip. 11 (2011) 2488–2492.

[10]   D.V.R. Kumar, M. Kasture, A.A. Prabhune, C. V. Ramana, B.L.V. Prasad, A.A. Kulkarni, Continuous flow synthesis of functionalized silver nanoparticles using bifunctional biosurfactants, Green Chem. 12 (2010) 609–615.

[11]   S. Seibt, P. Mulvaney, S. Förster, Millisecond CdS nanocrystal nucleation and growth studied by microfluidics with in situ spectroscopy, Colloids Surfaces A Physicochem. Eng. Asp. 562 (2019) 263–269.

[12]   S. Sofela, S. Sahloul, M. Rafeie, T. Kwon, J. Han, M.E. Warkiani, Y.A. Song, High-throughput sorting of eggs for synchronization of: C. elegans in a microfluidic spiral chip, Lab Chip. 18 (2018) 679–687.

[13]   Y. Gou, S. Zhang, C. Sun, P. Wang, Z. You, Y. Yalikun, Y. Tanaka, D. Ren, Sheathless Inertial Focusing Chip Combining a Spiral Channel with Periodic Expansion Structures for Efficient and Stable Particle Sorting, Anal. Chem. 9 (2019) A-I.

[14]   P. Kim, K.W. Kwon, M.C. Park, S.H. Lee, S.M. Kim, K.Y. Suh, Soft lithography for microfluidics: A Review, Biochip J. 2 (2008) 1–11.

[15]   J. Singh, N. Kockmann, K.D.P. Nigam, Novel three-dimensional microfluidic device for process intensification, Chem. Eng. Process. Process Intensif. 86 (2014) 78–89.

[16]   R.K. Thakur, C. Vial, K.D.P. Nigam, E.B. Nauman, G. Djelveh, Static mixers in the process industries - a review, Chem. Eng. Res. Des. 81 (2003) 787–826.

[17]   N. Kockmann, D.M. Roberge, Transitional flow and related transport phenomena in curved microchannels, Heat Transf. Eng. 32 (2011) 595–608.

[18]   S. Horikoshi, T. Sumi, N. Serpone, A Hybrid Microreactor/Microwave High-Pressure Flow System of a Novel Concept Design and its Application to the Synthesis of Silver Nanoparticles, Chem. Eng. Process. Process Intensif. 73 (2013) 59–66.

[19]   Y. Maralla, S. Sonawane, Process intensification using a spiral capillary microreactor for continuous flow synthesis of performic acid and it's kinetic study, Chem. Eng. Process. - Process Intensif. 125 (2018) 67–73.

[20]   Y. Maralla, S.H. Sonawane, Process intensification by using a helical capillary microreactor for a continuous flow synthesis of peroxypropionic acid and its kinetic study, Period. Polytech. Chem. Eng. 64 (2020) 9–19.

[21]   L. Gutierrez, L. Gomez, S. Irusta, M. Arruebo, J. Santamaria, Comparative study of the synthesis of silica nanoparticles in micromixer-microreactor and batch reactor systems, Chem. Eng. J. 171 (2011) 674–683.

[22]   Zhuravlev.L T, The surface chemistry of amorphous silica. Zhuravlev model, Colloids Surfaces A Physicochem. Eng. Asp. 173 (2000) 1–38.

[23]   N. Plumeré, A. Ruff, B. Speiser, V. Feldmann, H.A. Mayer, Stöber silica particles as basis for redox modifications: Particle shape, size, polydispersity, and porosity, J. Colloid Interface Sci. 368 (2012) 208–219.

[24]   Y. Ohtsu, H. Fukui, T. Kanda, K. Nakamura, M. Nakano, O. Nakata, Y. Fujiyama, Structures and chromatographic characteristics of capsule-type silica gels coated with

hydrophobic polymers in reversed-phase liquid chromatography, Chromatographia. 24 (1987) 380–384.

[25] N. Hao, Y. Nie, A. Tadimety, T. Shen, J.X.J. Zhang, Microfluidics-enabled rapid manufacturing of hierarchical silica-magnetic microflower toward enhanced circulating tumor cell screening, Biomater. Sci. 6 (2018) 3121–3125.

[26] M.A. Khairul, R. Saidur, M.M. Rahman, M.A. Alim, A. Hossain, Z. Abdin, Heat transfer and thermodynamic analyses of a helically coiled heat exchanger using different types of nanofluids, Int. J. Heat Mass Transf. 67 (2013) 398–403.

[27] Y. Maralla, S. Sonawane, D. Kashinath, M. Pimplapure, B. Paplal, Process Intensification of Tetrazole reaction through tritylation of 5-[4'-(Methyl) Biphenyl-2-Yl] using microreactors, Chem. Eng. Process. Process Intensif. 112 (2017) 9–17.

[28] S.K. Kurt, M.G. Gelhausen, N. Kockmann, Axial Dispersion and Heat Transfer in a Milli/Microstructured Coiled Flow Inverter for Narrow Residence Time Distribution at Laminar Flow, Chem. Eng. Technol. 38 (2015) 1122–1130.

[29] Z. Liu, F. Fontana, A. Python, J.T. Hirvonen, H.A. Santos, Microfluidics for Production of Particles: Mechanism, Methodology,and Applications, Small. 1904673 (2019) 1–24.

[30] C.K. Dixit, S. Bhakta, A. Kumar, S.L. Suib, J.F. Rusling, Fast nucleation for silica nanoparticle synthesis using a sol-gel method, Nanoscale. 8 (2016) 19662–19667.

[31] R.S. Fernandesa, I.M.R. Jr., M.F. Pimentel, Revising the synthesis of Stöber silica nanoparticles: A multivariate assessment study on the effects of reaction parameters on the particle size, Colloids Surfaces A. 577 (2019) 1–7.

[32] R. Lindberg, G. Sundholm, B. Pettersen, J. Sjoblom, S.E. Friberg, Multivariate analysis of the size dependence of monodisperse silica particles prepared according to the sol-gel technique, Colloids Surfaces A. 123–124 (1997) 549–560.

[33] G.H.Bogush, M.A.Tracy, C.F.Zukoskiiv, Preparation of monodisperse polyisobutene

grafted silica dispersion, Colloids and Surfaces. 34 (1988) 81–88.

[34] K. Nozawa, H. Gailhanou, L. Raison, P. Panizza, H. Ushiki, E. Sellier, J.P. Delville, M.H. Delville, Smart control of monodisperse stöber silica particles: Effect of reactant addition rate on growth process, Langmuir. 21 (2005) 1516–1523.

[35] S.K. Park, K. Do Kim, H.T. Kim, Preparation of silica nanoparticles: determination of the optimal synthesis conditions for small and uniform particles, Colloids Surfaces A. 9 (2016) 377–383.

[36] X.D. Wang, Z.X. Shen, T. Sang, X. Bin Cheng, M.F. Li, L.Y. Chen, Z.S. Wang, Preparation of spherical silica particles by Stöber process with high concentration of tetra-ethyl-orthosilicate, Colloid Interface Sci. 341 (2010) 23–29.

TOC Graphic
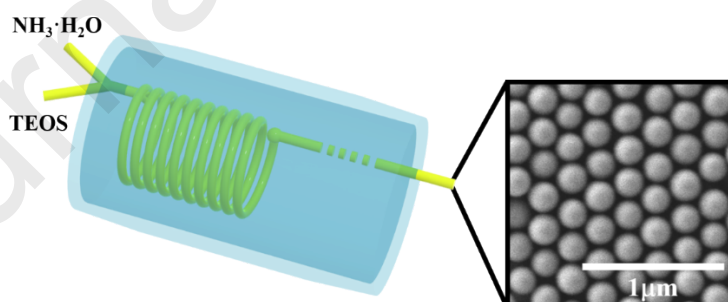
Supplementary Information

A lithography free microfluidic device for the high throughput synthesis of monodisperse silica nanoparticles

Hui Yang[1,2], Eser Metin Akinoglu[3,1], Lijing Guo[1], Mingliang Jin[1], Guofu Zhou[1,2], Michael Giersig[1,4], Lingling Shui[1,5], Paul Mulvaney[3,1]
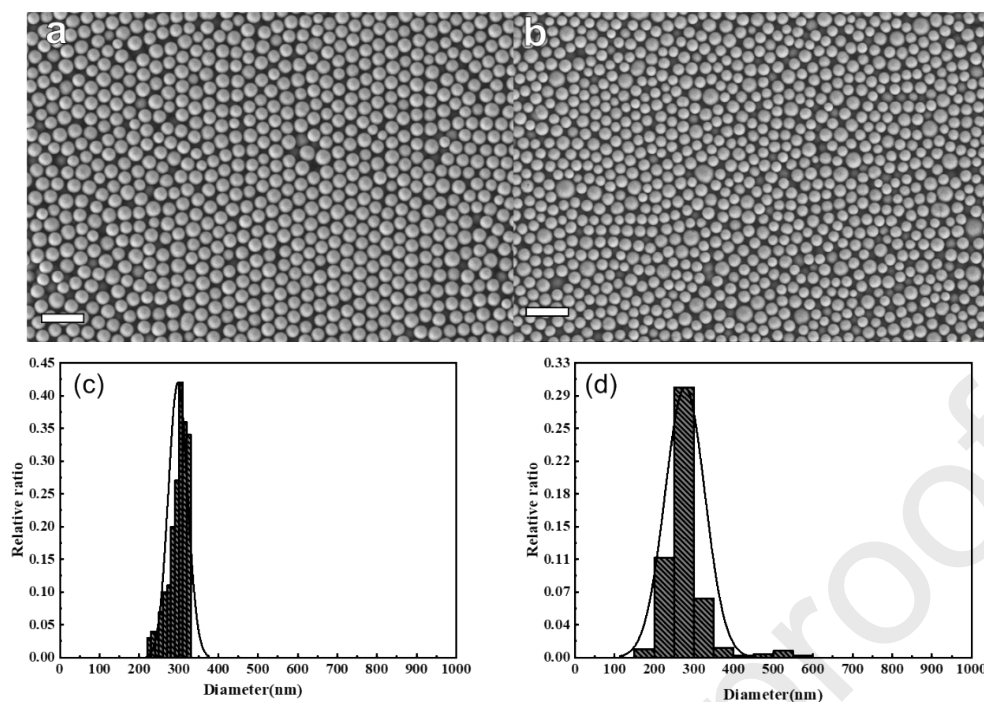
[1] *International Academy of Optoelectronics at Zhaoqing, South China Normal University, Zhaoqing, 526238 Guangdong, P. R. China*

[2] *Guangdong Provincial Key Laboratory of Optical Information Materials and Technology & Institute of Electronic Paper Displays, South China Academy of Advanced Optoelectronics, South China Normal University, Guangzhou 510006, P.R. China*

[3] *ARC Centre of Excellence in Exciton Science, School of Chemistry, University of Melbourne, Parkville, VIC, 3010, Australia*

[4] *Institute of Fundamental Technological Research, Polish Academy of Sciences, 02-106 Warsaw, Poland*

[5] *School of Information and Optoelectronic Science and Engineering, South China Normal University, Guangzhou, 510006 Guangdong, P. R. China*
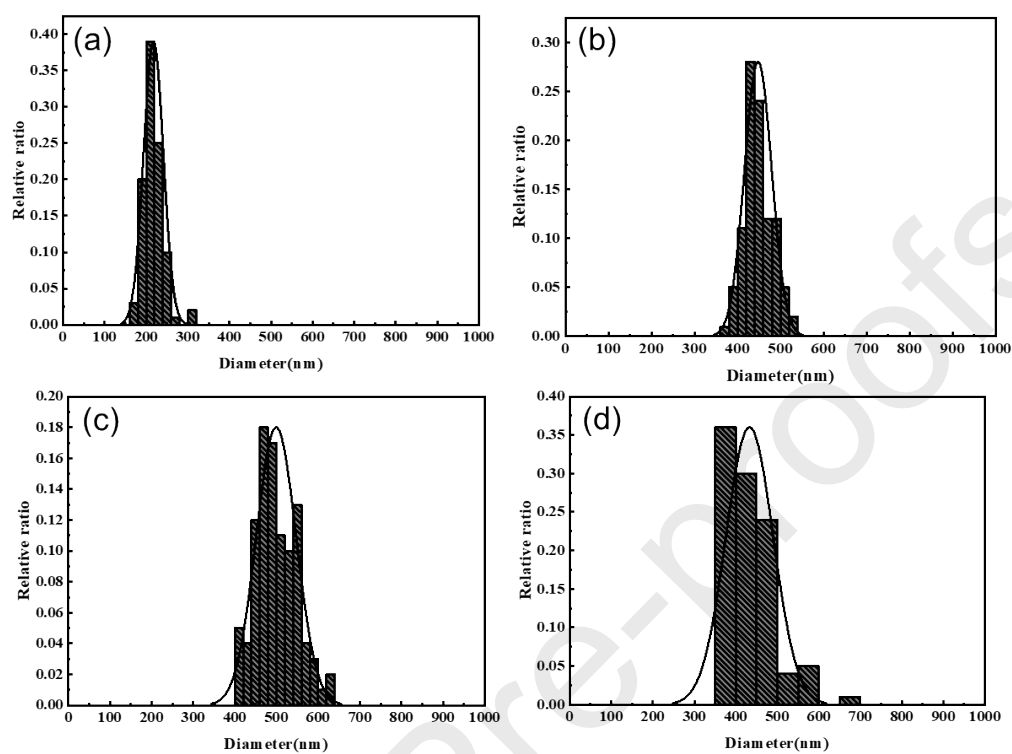
Figure S1. Sem images of SiO$_2$ particles. (a) and (c) with micromixer, (b) and (d) without micromixer. The scale bar is 1 μm.
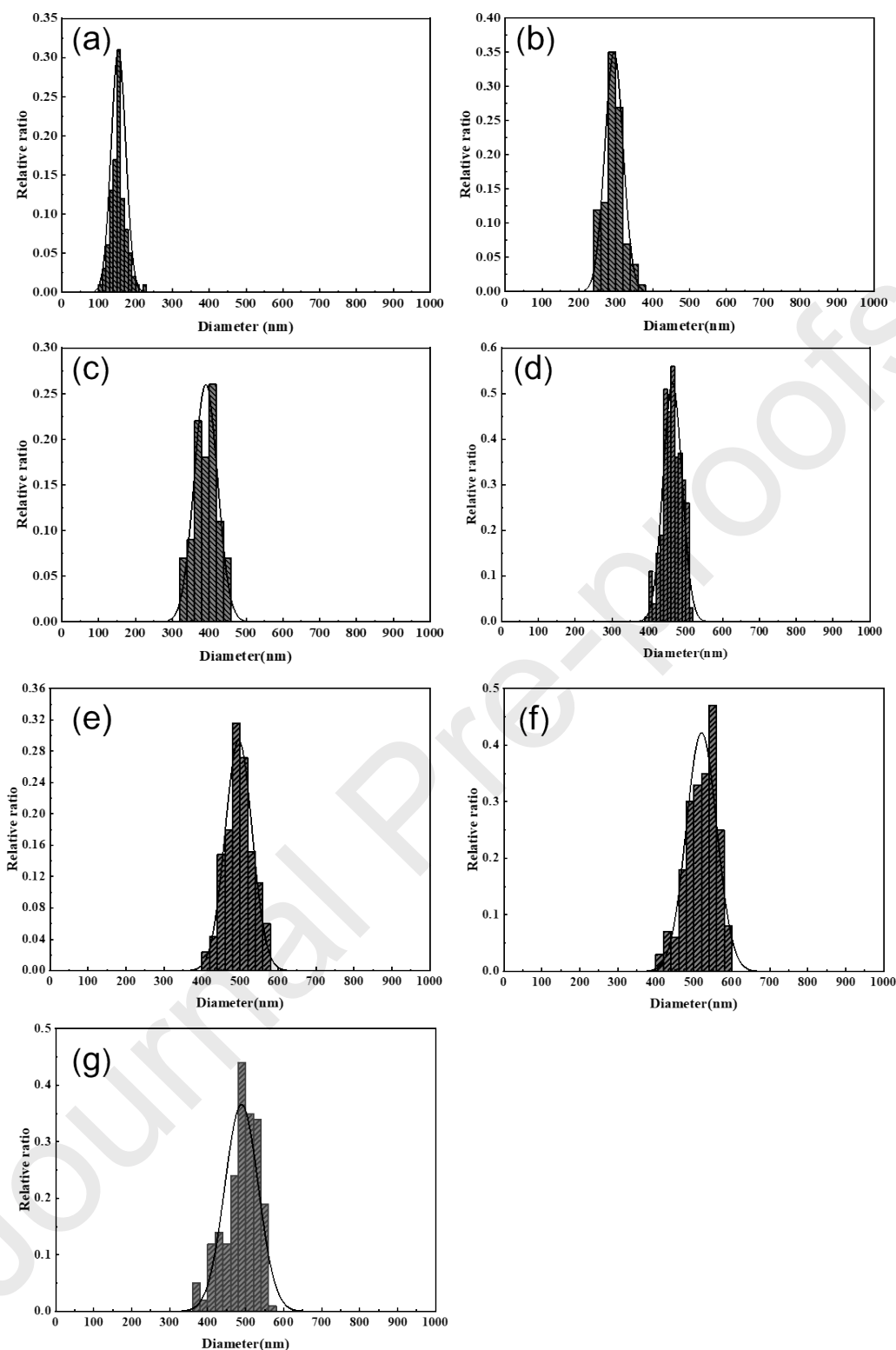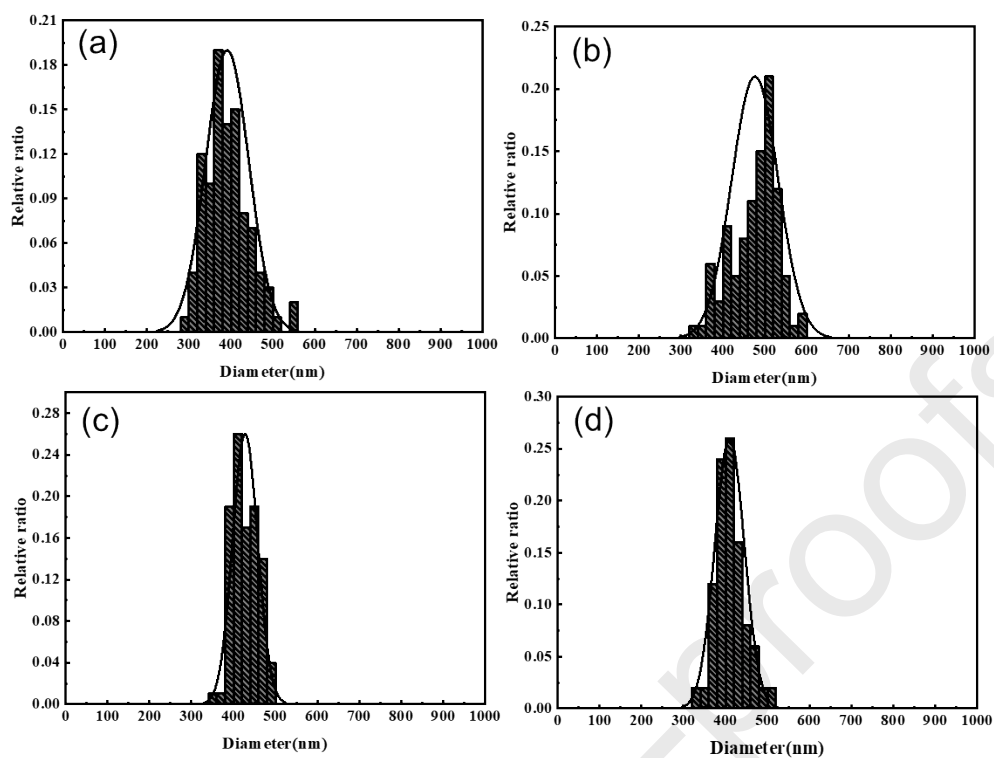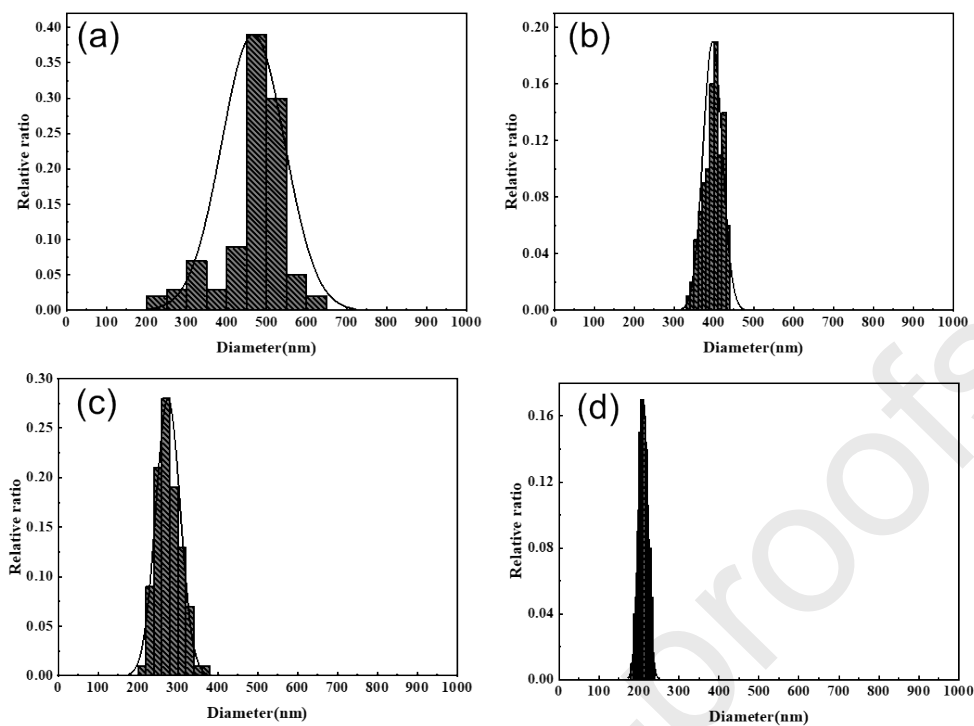
Figure S2. Histograms showing the size distributions of the SiO$_2$ NPs obtained at different TEOS

concentrations (a) 0.013 mol/L, (b)0.13 mol/L, (c) 0.26 mol/L, (d) 0.39 mol/L, (e) 0.52 mol/L, (f) 0.65 mol/L

and (g) 0.78 mol/L.

Figure S3. Histograms showing the size distribution of the SiO$_2$ NPs obtained at different NH$_3$

concentrations (a) 4.35 mol/L, (b) 8.7 mol/L, (c) 13.05 mol/L, and (d) 17.4 mol/L.

Figure S4. Histograms showing the size distribution of the SiO$_2$ NPs obtained at different flow rates (a) 200 μL/min, (b) 300 μL/min, (c) 400 μL/min, and (d) 500 μL/min.

Figure S5. Histograms showing the size distribution of the SiO$_2$ NPs obtained at different temperatures (a) 30 °C, (b) 40 °C, (c) 50 °C, and (d) 60 °C.
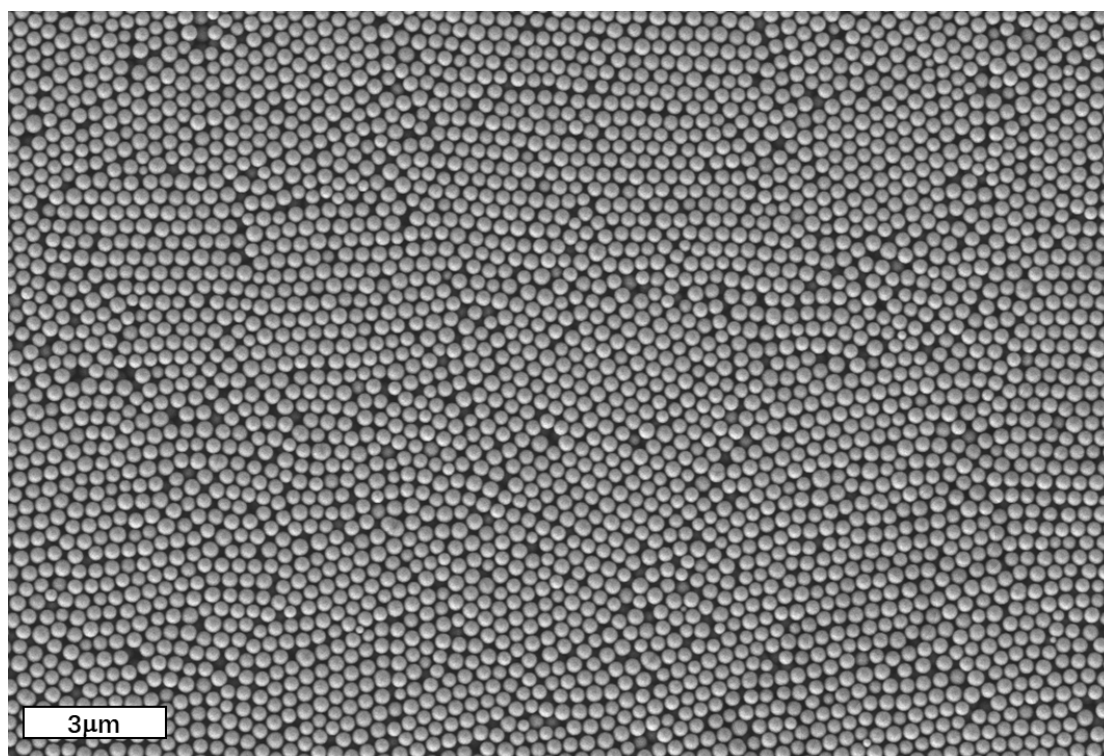
Figure S6. Large view SEM image of SiO$_2$ particles. c_{TEOS} = 0.13 mol/L, c_{NH3} = 8.7 mol/L, T = 40 °C, and the flow rate at 400 µL/min.

Highlights

- Continuous flow SiO$_2$ nanoparticle synthesis using a helical capillary microreactor
- Dean flow mediated ultrafast mixing
- Particle size control between 100 nm and 600 nm and narrow polydispersity

- Very stable suspensions even at high particle volume fractions
- Yield of 0.234 g/h of the silica particles